Magnetization steps in the molecular magnet Ni_4Mo_{12} revealed by complex exchange bridges

M. Georgiev [*] and H. Chamati [†]

Institute of Solid State Physics, Bulgarian Academy of Sciences, Tsarigradsko Chaussée 72, 1784 Sofia, Bulgaria

(Received 23 July 2019; revised manuscript received 2 March 2020; accepted 4 March 2020; published 20 March 2020)

We study the behavior of the magnetization and the magnetic susceptibility of molecular magnets with complex bridging structure. Our computations are based on a post-Hartree-Fock method accounting for the intricate network of interatomic bonds and an effective spinlike Hamiltonian that captures the essential magnetic features of magnetic molecules. The devised method and the constructed Hamiltonian are further employed to characterize the magnetic properties of the molecular magnet Ni_4Mo_{12}. The obtained results reproduce both quantitatively and qualitatively the main features of the magnetic spectrum. Furthermore, the computations for the magnetization and the low-field susceptibility are in very good agreement with their experimental counterparts. In this respect, they improve upon the results obtained with conventional Heisenberg models.

DOI: 10.1103/PhysRevB.101.094427

I. INTRODUCTION

Molecular magnets are some of the most prominent examples of physical systems that unveil the quantum origin of magnetism. Due to their plain chemical structure and small number of constituent ions, nanomagnets demonstrate peculiar magnetic and related properties that underpin future applications [1–6] and challenge scientists working in different fields.

The effects observed in Mn_{12} acetate [7–12], Fe_8-based molecular magnets [13–16], and in the Ni_4 clusters [17–21], strongly emphasize the unique role of nanomagnets in determining the relation between electrons' correlations and magnetism. On the molecular level the existing magnetic exchange processes uniquely characterize the nanomagnets' properties [21,22]. The number and type of constituting elements, their bonding, and thus the resulting geometric symmetry lies in the footprints of each nanomagnet, such as the lightly distorted octahedral magnetic molecules with a central Cr ion [23], the high spin molecular complex Fe_{19} [24], the molecular wheel Fe_{18} [25] with 18 antiferromagnetically coupled spin-$\frac{5}{2}$ ions, and the heterometalic Cr_7Ni antiferromagnet [26–28]. Despite the fact that in addition to the above-mentioned compounds a huge variety of molecular magnets (see, e.g., Refs. [29–38] and references therein) were synthesized and extensively studied during the last decade, one could still be fascinated by the richness of their magnetic properties and the challenges they pose to scientists.

The intricate magnetic features of the molecule $[Mo_{12}O_{30}(\mu_2\text{-OH})_{10}H_2(Ni(H_2O)_3)_4]$ (Ni_4Mo_{12}), with four Ni magnetic centers occupying the vertices of a slightly distorted tetrahedron [39], has been the subject of many investigations [18–21]. In Ref. [19], a very general Heisenberg model involving different sorts of magnetic interactions among localized spins and the Hubbard model with localized electrons were used to analyze INS data. Both studied models were proven unable to appropriately explain the magnetism in the named molecular magnets. Further analysis of the magnetic spectra of Ni_4Mo_{12}, formulated as $[Mo_{12}O_{28}(\mu_2\text{-OH})_9(\mu_3\text{-OH})_3(Ni(H_2O)_3)_4]$, was performed in Ref. [20], where in terms of the Heisenberg model a naive spin coupling scheme with two arbitrary coupling parameters of the isotropic Heisenberg model was used. The physical reason lying behind this parametrization was not discussed. A shortcoming of the proposed model is that it provides a single intensity curve for all three low-temperature magnetic peaks. Moreover, even after including a single-ion anisotropy with yet another running parameter, the magnetic features of Ni_4Mo_{12} could not be fully determined. A more recent study [21] showed that electron correlations are the driving mechanisms behind magnetism of four-center transition-metal clusters. Thus, despite the efforts an overall theoretical description and deep understanding of the magnetic spectrum obtained via inelastic neutron scattering (INS) experiments is still an open question.

In an attempt to elucidate the mechanisms underpinning the magnetic properties of this molecule we revisited the reported experimental data and proposed an alternative approach [40–42] that helped explain the details of the magnetic spectrum obtained via INS, see Fig. 1. Within our approach the four magnetic excitations, I, II, III, and IV, with energies $\Delta_{\rm I} = 0.4$, $\Delta_{\rm II} = 0.6$, $\Delta_{\rm III} = 1.7$, and $\Delta_{\rm IV} = 1.15$ meV, and INS intensities I_{10}, I_{30}, I_{50}, and I_{64}, respectively, are uniquely characterized. All features in the magnetic spectrum, such as splitting and broadening, were revealed. For further details the reader may consult Ref. [42].

In order to interpret the experimental measurements of the magnetization and the susceptibility obtained for Ni_4Mo_{12} reported in Ref. [17], the authors relied on electron paramagnetic resonance measurements and explored the relevant magnetooptical properties. They combined the isotropic Heisenberg Hamiltonian with a biquadratic and a

[*] mgeorgiev@issp.bas.bg
[†] chamati@issp.bas.bg

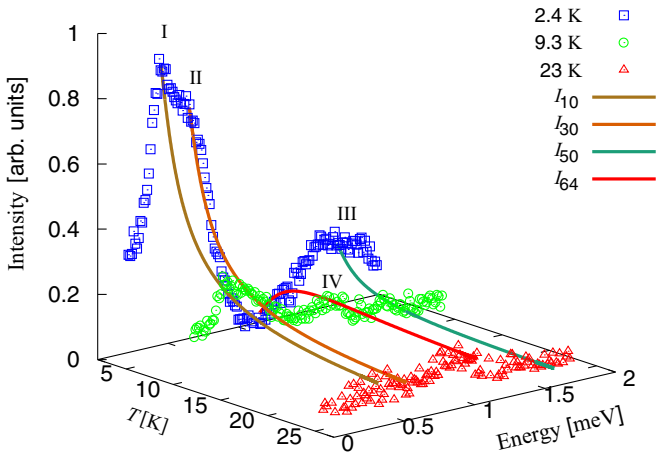

FIG. 1. Inelastic neutron scattered intensities for the magnetic molecule Ni_4Mo_{12} as a function of the temperature and neutrons' energy transfer. The experimental data are taken from Ref. [19]. The curves represent the calculated intensities $I_{n'n}$, with n and n' denoting the number of initial and final states in the transition processes, where $n = 0$ is the ground state.

single-ion anisotropy terms in addition to field-dependent coupling parameters. This allowed them to qualitatively reproduce the magnetization and susceptibility measurements data but failed to explain the inelastic neutron scattering experiments [19]. Another study of the magnetization and the susceptibility [18] proposed a non-negligible contribution of the three-body spin interaction term. To reproduce the behavior of the field-dependent magnetization and the associated susceptibility of the compound under consideration, it was suggested [20] to account for single-ion anisotropy, as well. However, no firm physical grounds were reported in support of the pure technical procedure leading to the parametrization of Ref. [20]. Furthermore it does not account for the background emanating from delocalized electrons.

In this paper we report theoretical results on the magnetization and the magnetic susceptibility results for the tetramer Ni_4Mo_{12} based on the proposed in Ref. [42] spinlike Hamiltonian taking into account the Zeeman term. From the physical point of view the present model opens a new perspective on the theoretical studies of the magnetic spectrum, magnetization and magnetic susceptibility of Ni_4Mo_{12}. Notice that in contrast to the introduced in Ref. [20] picture of strongly localized electrons, the model considered in this paper views the electrons as delocalized and hence assures the role of the bridging structure in the exchange processes. This is in concert with other investigations on clusters with four Ni centers [18,19,21,42]. We would like to anticipate that the obtained results are in good qualitative and fairly quantitative agreement with the corresponding experimental measurements data [17]. The analysis suggests that the observed shifting in magnetization steps is associated to variations in the correlations between delocalized electrons due to the presence of externally applied magnetic field. The influence of the field is indirect and differs by a contribution emanating from the Zeeman term. It originates from the interaction between the molecules intrinsic magnetic vector potential and the magnetic vector potential of the external field, and it is especially underlined due to the electrons' delocalization. The resulting interaction terms contribute to the correlation functions derived from a post-Hartree-Fock method and thus enters into the spinlike Hamiltonian. Moreover, the approach proposed here leads to improvements upon that based on the conventional isotropic Heisenberg model. For the sake of comparison we computed the magnetization and magnetic susceptibility with the aid of the isotropic Heisenberg model, as well as the Hamiltonian involving anisotropic in space spin-spin interaction and an axial single-ion anisotropy proposed in Ref. [20].

The rest of this paper is organized as follows. In Sec. II A we write down the Hamiltonian and the model parameters relevant to the present study. In Sec. III we obtain the explicit expression of the energy spectrum as a function of all running parameters used to study the magnetization and the magnetic susceptibility of the Ni_4Mo_{12}. In Sec. III C we determine the values of the model parameters fitted to the experimental results. A summary of the results obtained throughout this paper is presented in Sec. IV.

II. EFFECTIVE MODEL

A. Spinlike Hamiltonian

In order to investigate the magnetic properties of the tetramer we apply the formalism presented in Ref. [42] by accounting for the action of the externally applied magnetic field. Thus, we consider the following spinlike Hamiltonian:

$$\hat{\mathcal{H}} = \sum_{i \neq j} J_{ij} \hat{\boldsymbol{\sigma}}_i \cdot \hat{\mathbf{s}}_j - \mu_B B \sum_i g_i^{\alpha} \hat{s}_i^{\alpha}, \tag{2.1}$$

where $J_{ij} = J_{ji}$ are effective constants, the operator $\hat{\boldsymbol{\sigma}}_i = (\hat{\sigma}_i^x, \hat{\sigma}_i^y, \hat{\sigma}_i^z)$ indirectly accounts for the differences in electrons' distribution with respect to the ith magnetic center with spin operator $\hat{\mathbf{s}}_i$, μ_B is the Bohr magneton, g_i^{α} is the α component of the corresponding effective g factor and B is the magnitude of the external magnetic field oriented along a preselected magnetic easy axis $\alpha \in \{x, y, z\}$. Moreover, for each total spin multiplet the σ operators will also account for the rate at which the electrons' correlations alter due to the presence of an externally applied magnetic field.

We would like to point out that the effective g factor differs from the g tensor known in the theory of magnetism. Thus, in contrast to the widely applied g tensor, derived via the quantum perturbation theory, the effective g factor resulting from the post-Hartree-Fock method is a three-component vector $\mathbf{g}_i = (g_i^x, g_i^y, g_i^z)$. The reason is that we use a variational method and the electrons are regarded as delocalized to a large extent, occupying molecular orbitals. The technical details behind the derivation of $\mathbf{g}$ vector lies beyond the objective of the present paper and will be a subject of separate paper [43]. However, following the short review in Ref. [42] explaining the main steps leading to the construction of the spin-sigma bilinear form in (2.1) we can give an explicit representation of the effective g factor.

It is worth mentioning that the applied formalism is based on a multiconfiguration self-consistent field method [44–46] that in turn relies on the molecular orbital theory [47,48] as

the main approach in describing the interatomic bonding. The initial canonical Hamiltonian that leads to (2.1) takes into account the electrons' kinetic energy, the electron-electron and electron-nuclei interactions, in addition to the influence of externally applied magnetic field on the electrons' motion. In addition to the action of the external magnetic field, each electron is viewed as interacting with an intrinsic local magnetic field that originates from the orbital and spin angular momenta of all remaining electrons. All electrons in the system are considered as delocalized in terms of the molecular orbital theory. Thus, they occupy molecular orbitals $\phi_{n,m_i}(\mathbf{r}_i)$, with $n \in \mathbb{N}$, represented as a linear combination of atomic orbitals $\psi^{\eta}_{\mu_{\eta i},m_i}(\mathbf{r}_i)$, where $\mathbf{r}_i$ are the coordinates of the ith electron, $\mu_{\eta i}$ denotes the electronic shell and subshell with respect to the η nucleus and ith electron, m_i is the spin magnetic quantum number of the ith electron. In the considered method, different exchange bridges may favor different electrons' distributions and thus configurations. Therefore, the corresponding state functions are given by a linear combination of Slater determinants with elements $\phi_{n,m_i}(\mathbf{r}_i)$ and are symmetrized in accordance to the spin quantum numbers s_{ij} of all electron pairs and with respect to all probable electrons' distributions along all exchange bridges.

Within the assumption of delocalized electrons the effective g factor may be derived from the interaction between the magnetic vector potential of the externally applied field and the magnetic vector potentials associated to the orbital and spin magnetic moments of the constituent electrons. These interactions result from the relevant electrons' generalized momenta. In terms of N electrons with $N-2$ pairs, the effective g factor associated with the $(N-1)$th and Nth unpaired by orbitals electrons is given by

$$g_\alpha = \frac{1}{2}\sum_\tau |c_\tau|^2\left(g^{\alpha,\tau}_{N-1} + g^{\alpha,\tau}_{N}\right),$$

where the coefficient c_τ accounts for the probability of observing both electrons in one of the three possible triplet configurations associated with a set of molecular orbitals $\tau = (n, \ldots, n')$, with n denoting the orbital's number. Further, for all $\alpha \in \{x, y, z\}$ we have

$$g^{\alpha,\tau}_N = g_e n_\alpha - g_e \frac{e^2\mu_0}{8\pi^2 m_e}\sum_{j=1}^{N-1}\left\langle \frac{\alpha_j(\mathbf{n}\cdot\mathbf{r}_{Nj}) - n_\alpha(\mathbf{r}_j\cdot\mathbf{r}_{Nj})}{r^3_{Nj}}\right\rangle_\tau,$$

where g_e is the electron's spin g factor, e is the elementary charge, μ_0 is the magnetic permeability, m_e is the electron's rest mass, $\mathbf{n} = (n_x, n_y, n_z)$ is a unit vector such that $B = \mathbf{n}\cdot\mathbf{B}$, $\mathbf{r}_j = (x_j, y_j, z_j)$ are the coordinates of the jth electron, and r_{Nj} is the distance separating the Nth and the jth electrons.

B. Properties of the σ operators

For the sake of completeness, we present the properties of σ operators relevant to the present study. Additional details can be found in Refs. [40,42].

The components of σ operator are such that for all i and $\alpha \in \{x, y, z\}$, we have

$$\hat{\sigma}^\alpha_i|\ldots, s_i, m_i, \ldots\rangle = a^{s_i,m_i}_i \hat{\mathrm{s}}^\alpha_i\,|\ldots, s_i, m_i, \ldots\rangle, \tag{2.2}$$

where $a^{s_i,m_i}_i \in \mathbb{R}$.

When the ith and jth spin centers are coupled, with total spin operator $\hat{\mathbf{s}}_{ij} = \hat{\mathbf{s}}_i + \hat{\mathbf{s}}_j$, one has the corresponding total σ operator $\hat{\boldsymbol{\sigma}}_{ij}$. Hence, similar to Eqs. (2.2), for all $i \neq j$ and $\alpha \in \{x, y, z\}$, we have

$$\hat{\sigma}^\alpha_{ij}|\ldots, s_{ij}, s, m\rangle = a^{s,s_{ij},m_{ij}}_{ij}\hat{\mathrm{s}}^\alpha_{ij}\,|\ldots, s_{ij}, s, m\rangle, \tag{2.3}$$

where $a^{s,s_{ij},m_{ij}}_{ij} \in \mathbb{R}$. The individual σ operators from the (i, j)th spin pair share the same coefficient. Thus, for any $i \neq j$ and $\alpha \in \{x, y, z\}$ one gets

$$\hat{\sigma}^\alpha_i|\ldots, s_{ij}, s, m\rangle = a^{s,s_{ij},m_{ij}}_{ij}\hat{\mathrm{s}}^\alpha_i\,|\ldots, s_{ij}, s, m\rangle. \tag{2.4}$$

In the presence of an external magnetic field the constraints in Ref. [42], obtained without magnetic field need to be modified. Since according to the underlying post-Hartree-Fock method the electrons' correlations are field dependent, in the considered case these constraints enter a more general form. The equations relating σ and spin operators read

$$\hat{\sigma}^z_{ij}|\ldots, s_{ij}, s, m\rangle = h^s_{ij}\,\hat{\mathrm{s}}^z_{ij}|\ldots, s_{ij}, s, m\rangle, \tag{2.5a}$$

$$\hat{\boldsymbol{\sigma}}^2_{ij}|\ldots, s_{ij}, s, m\rangle = \left(h^s_{ij}\right)^2 s_{ij}(s_{ij}+1)|\ldots, s_{ij}, s, m\rangle, \tag{2.5b}$$

where the parameter $h^s_{ij} \in \mathbb{R}$ accounts for the changes in electrons' correlations due to the indirect action of the externally applied magnetic field. Such an influence alters the energy spectrum obtained for $B = 0$ and differs from the contribution associated to the Zeemen term. Notice that in the absence of external magnetic field, for all s and s_{ij} one has $h^s_{ij} = 1$.

Using Eqs. (2.3) and the constraints (II.5) we distinguish four cases:

(i) For $s_{ij} \neq 0$ and $m_{ij} \neq 0$, or when the value of m_{ij} cannot be determined, we have $a^{s,s_{ij},m_{ij}}_{ij} = h^s_{ij}$.

(ii) When $s_{ij} \neq 0$ and $m_{ij} = 0$, then from Eq. (2.5b) it follows that

$$a^{s,s_{ij},0}_{ij} = \pm h^s_{ij}. \tag{2.6}$$

(iii) In the presence of a singlet bond, $s_{ij} = 0$, one has unconstrained parameters such that for the set of coefficients $c^n_{ij} \in \mathbb{R}$,

$$a^{s,0,0}_{ij} \in \left\{h^s_{ij}c^n_{ij}\right\}_{n\in\mathbb{N}}. \tag{2.7}$$

(iv) In the case of a total singlet $s = 0$ and $s_{ij} = 0$ the system resemble a closed shell system with unique electron configuration. As a result, the effective parameter will have a unique value

$$a^{0,0,0}_{ij} = h^0_{ij}. \tag{2.8}$$

For more details on the quantities c^n_{ij} see Ref. [42]. In general, within Hamiltonian (2.1) one relies on two classes of parameters. The spectroscopic parameters c^n_{ij} that can be fitted according to performed spectroscopic measurements and the parameters h^s_{ij} that account for the effect of externally applied magnetic filed. The latter can be fixed with respect to the magnetization and magnetic susceptibility measurements.

III. Ni_4Mo_{12}

A. Hamiltonian

The spin-sigma bilinear form in (2.1) is derived in a such a way to be valid for arbitrary magnetic field. Therefore, for calculating the energy spectrum for $B \neq 0$, we take into account the applied spin coupling scheme discussed in Ref. [42]. In other words we have Ni1-Ni2 and Ni3-Ni4 spin bonds and the eigenstates $|s_{12}, s_{34}, s, m\rangle$. Since the four Ni spin centers are indistinguishable, for $i, j = 1, \ldots, 4$ we set $J_{ij} = J$. Furthermore, we distinguish two σ bond operators, $\hat{\boldsymbol{\sigma}}_{12}$ and $\hat{\boldsymbol{\sigma}}_{34}$, corresponding to Ni1-Ni2 and Ni3-Ni4 spin pairs, respectively. According to (2.3) and (2.4) one has the spin bond parameters $a_{12}^{s,s_{12},m_{12}}$ and $a_{34}^{s,s_{34},m_{34}}$ associated with Ni1-Ni2 and Ni3-Ni4 spin pairs, respectively. In our previous work [42], with the aid of the spectroscopic parameters c_{12} and c_{34}, see also (2.7), we were able to unveil the driving exchange mechanism behind the magnetic spectrum of Ni_4Mo_{12}. Now, taking in to account the field parameters h_{12}^s and h_{34}^s we can shed more light on the way the external magnetic field affect the electrons' correlations in this magnetic molecule.

Using (2.1) and selecting the z axis as the magnetic easy axis we end up with the Hamiltonian

$$\begin{aligned}\hat{\mathcal{H}} = &J(\hat{\boldsymbol{\sigma}}_1 \cdot \hat{\mathbf{s}}_2 + \hat{\boldsymbol{\sigma}}_2 \cdot \hat{\mathbf{s}}_1 + \hat{\boldsymbol{\sigma}}_3 \cdot \hat{\mathbf{s}}_4 + \hat{\boldsymbol{\sigma}}_4 \cdot \hat{\mathbf{s}}_3) \\ &+ J(\hat{\boldsymbol{\sigma}}_{12} \cdot \hat{\mathbf{s}}_{34} + \hat{\boldsymbol{\sigma}}_{34} \cdot \hat{\mathbf{s}}_{12}) - g\mu_B B\, \hat{\mathbf{s}}^z, \end{aligned} \tag{3.1}$$

where $\hat{\mathbf{s}}^z$ is the total spin z component and since all Ni centers are indistinguishable for $i = 1 \ldots, 4$ we may set $g = g_i^z$.

With the aid of Hamiltonian (3.1) the total spin s remains a good quantum number and hence the magnetic molecule is fully described by a total of 81 eigenstates.

B. Energy spectrum

Bearing in mind that the model parameters $a_{12}^{s,s_{12},m_{12}}$ and $a_{34}^{s,s_{34},m_{34}}$ take discrete values, the energy spectrum of Hamiltonian (3.1) can be generalized by the expression

$$\begin{aligned}E_{s_{12},s_{34},s}^m = &Ja_{12}^{s,s_{12},m_{12}}[s_{12}(s_{12}+1) - 2s_0(s_0+1)] \\ &+ Ja_{34}^{s,s_{34},m_{34}}[s_{34}(s_{34}+1) - 2s_0(s_0+1)] \\ &+ \tfrac{1}{2}J\left(a_{12}^{s,s_{12},m_{12}} + a_{34}^{s,s_{34},m_{34}}\right)[s(s+1) - s_{12}(s_{12}+1) \\ &- s_{34}(s_{34}+1)] - g\mu_B Bm. \end{aligned} \tag{3.2}$$

The eigenvalues in (3.2) are not explicit functions of the scalars in (2.7). However, for convenience their dependence on the number n will be explicitly underlined only in the case when $n > 1$.

According to Ref. [42] and the analysis based on the inelastic neutron scattering experiments reported in Refs. [19,20] the ground state of this nanomagnet appears to be the singlet $|1, 1, 0, 0\rangle$. Taking into account (2.5) for the ground-state energy, we obtain

$$E_{1,1,0}^0 = E_{2,2,0}^0 = E_{0,0,0}^0 = -4J\left(h_{12}^0 + h_{34}^0\right).$$

The triplet level is determined by eighteen eigenstates, where $|1, 1, 1, m\rangle$ and $|2, 2, 1, m\rangle$, with $m = 0, \pm 1$, are characterized by the energy

$$E_{2,2,1}^m = E_{1,1,1}^m = -3J\left(h_{12}^1 + h_{34}^1\right) - g\mu_B Bm.$$

TABLE I. The values of the model parameters used to characterize the magnetic properties of Ni_4Mo_{12}. The evaluation of the spectroscopic parameters J, c_{12}^1, c_{12}^2, and c_{34} is achieved within the neutron spectroscopy data of Ref. [42]. All "h" parameters are fitted in accordance to the experimental data from the magnetization measurements depicted on Fig. 3.

B [T]	0	0–4.5	4.5–8.9	8.9–20.1	20.1–32	>32
$M/g\mu_B$	0	0	1	2	3	4
J [meV]	0.325					
c_{12}^1	1.192					
c_{12}^2	1.115					
c_{34}	1.038					
h_{12}^0	1	0.945				
h_{34}^0	1	0.793				
h_{12}^1	1		0.758			
h_{34}^1	1		0.879			
h_{12}^2	1			−0.289		
h_{34}^2	1			0.315		
h_{12}^3	1				1.532	
h_{34}^3	1				2.347	
h_{12}^4	1					1.554
h_{34}^4	1					1.595

Further, the respective triplets $|1, 2, 1, m\rangle$ and $|2, 1, 1, m\rangle$ energies are

$$E_{1,2,1}^m = -3J\left(h_{12}^1 + h_{34}^1\right) - 2J\left(h_{12}^1 - h_{34}^1\right) - g\mu_B Bm,$$

$$E_{2,1,1}^m = -3J\left(h_{12}^1 + h_{34}^1\right) + 2J\left(h_{12}^1 - h_{34}^1\right) - g\mu_B Bm.$$

With $|0, 1, 1, m\rangle$ the Ni1-Ni2 coupled spin pair form a singlet. The set of constants c_{12}^n in (2.7) then can be determined in the limit of zero external magnetic field, corresponding to $h_{12}^1 = 1$. According to the estimations for the low-lying magnetic excitations [42], found to be consistent with inelastic neutron scattering experiments [19,20], we have $c_{12}^1 = 1.1923$ and $c_{12}^2 = 1.1153$, see, e.g., Table I. Therefore, with $m = m_{34}$ and $n = 1, 2$, for the positive sign in (2.6) we get

$$E_{0,1,1}^m(c_{12}^n) = -4Jc_{12}^n h_{12}^1 - 2Jh_{34}^1 - g\mu_B Bm \tag{3.3}$$

and for the negative sign,

$$E_{0,1,1}^0(c_{12}^n) = -4Jc_{12}^n h_{12}^1 + 2Jh_{34}^1. \tag{3.4}$$

Thus, for each $m \neq 0$ we get two energies since $n = 1, 2$ and for $m = 0$ we have four. On the other hand, when the Ni3-Ni4 spin pair is in the singlet state, i.e., the triplet is $|1, 0, 1, m\rangle$, then $m = m_{12}$ and the coefficient $a_{34}^{1,0,0} = h_{34}^1 c_{34}^n$. The analysis of Ni_4Mo_{12} magnetic spectrum was performed within the approximation $n = 1$, where the spectroscopic parameter $c_{34}^1 = c_{34} = 1.0384$. Consequently, accounting for the sign in (2.6) we get

$$E_{1,0,1}^m = -4Jc_{34}h_{34}^1 - 2Jh_{12}^1 - g\mu_B Bm$$

and

$$E_{1,0,1}^0 = -4Jc_{34}h_{34}^1 + 2Jh_{12}^1.$$

The graphical representation of the energy sequence for $B = 0$ is shown on Fig. 2.

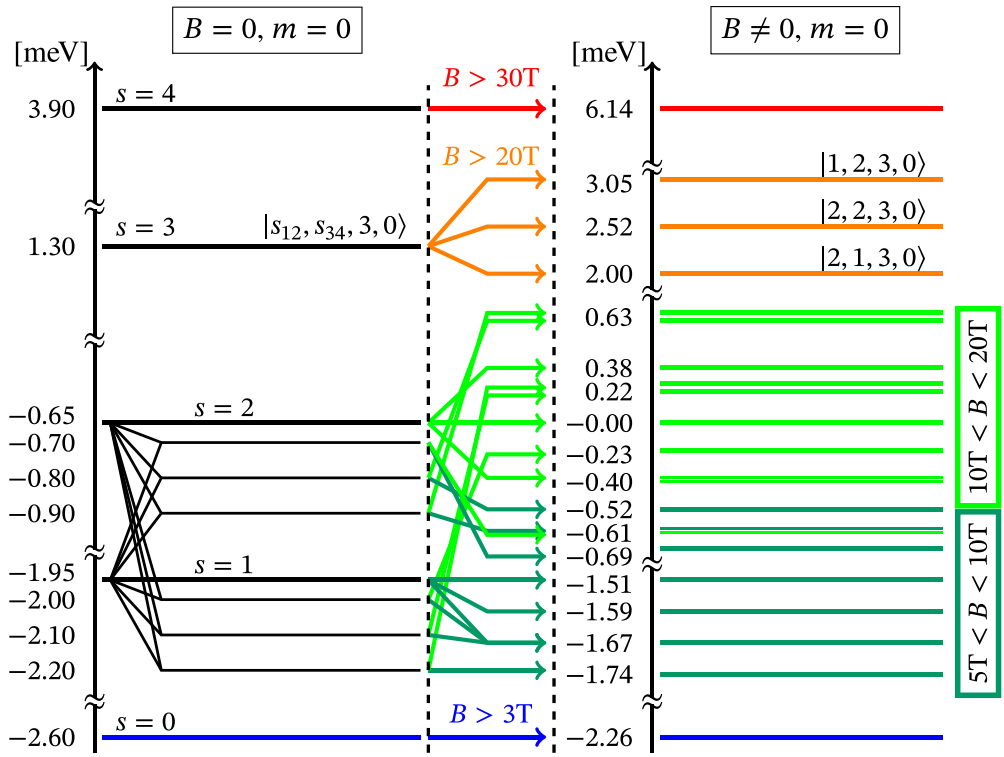

FIG. 2. Comparison between the energy spectra of Ni_4Mo_{12} for $B = 0$ on the left and $B \neq 0$ on the right assuming only the nonmagnetic states, $m = 0$. The blue and red colors mark the ground and higher-energy levels, respectively. The dark green lines depict the triplet, the green one stands for the quintet energy levels. Orange lines correspond to the septet energy levels. A detailed representation of the initial spectrum, placed on the left, is given in Ref. [42]. The domain between both dashed lines shows the splitting paths of the initial spectrum. The right-hand side spectrum is obtained according to the magnetization and susceptibility measurements reported in Ref. [17].

The quintet level is represented by 30 eigenstates and for $|1, 1, 2, m\rangle$ and $|2, 2, 2, m\rangle$, where $m = 0, \pm1, \pm2$ we obtain

$$E^m_{1,1,2} = E_{2,2,2} = -J\left(h^2_{12} + h^2_{34}\right) - g\mu_B Bm.$$

When the cluster exhibits the structure of a local triplet and quintet spin bonds with eigenstates $|1, 2, 2, m\rangle$ and $|2, 1, 2, m\rangle$ one obtains the following eigenvalues:

$$E^m_{1,2,2} = -J\left(h^2_{12} + h^2_{34}\right) - 2J\left(h^2_{12} - h^2_{34}\right) - g\mu_B Bm,$$

$$E^m_{2,1,2} = -J\left(h^2_{12} + h^2_{34}\right) + 2J\left(h^2_{12} - h^2_{34}\right) - g\mu_B Bm.$$

Similarly to (3.3) and (3.4) when the spins of Ni1-Ni2 ions are paired in a singlet $|0, 2, 2, m\rangle$, for the "+" sign in (2.6) one gets

$$E^m_{0,2,2}\left(c^n_{12}\right) = -4Jc^n_{12}h^2_{12} + 2Jh^2_{34} - g\mu_B Bm$$

and for the "−" sign

$$E^0_{0,2,2}\left(c^n_{12}\right) = -4Jc^n_{12}h^2_{12} - 2Jh^2_{34}.$$

For the Ni3-Ni4 singlet the eigenvalues are

$$E^m_{2,0,2} = -4Jc_{34}h^2_{34} + 2Jh^2_{12} - g\mu_B Bm$$

and

$$E^0_{2,0,2} = -4Jc_{34}h^2_{34} - 2Jh^2_{12}.$$

The septet level consists of twenty one eigenstates and in the presence of two quintet spin bonds, $|2, 2, 3, m\rangle$, one gets the energy

$$E^m_{2,2,3} = 2J\left(h^3_{12} + h^3_{34}\right) - g\mu_B Bm.$$

The eigenvalues of the remaining fourteen eigenstates $|1, 2, 3, m\rangle$ and $|2, 1, 3, m\rangle$ are given by

$$E^m_{1,2,3} = 2J\left(h^3_{12} + h^3_{34}\right) - 2J\left(h^3_{12} - h^3_{34}\right) - g\mu_B Bm,$$

$$E^m_{2,1,3} = 2J\left(h^3_{12} + h^3_{34}\right) + 2J\left(h^3_{12} - h^3_{34}\right) - g\mu_B Bm,$$

respectively. The indirect splitting of the septet level related with the inequality $h^3_{12} \neq h^3_{34}$ is depicted on Fig. 2.

All nonet eigenstates $|2, 2, 4, m\rangle$, with total magnetic quantum numbers $m = 0, \pm1, \pm2, \pm3, \pm4$, correspond to the eigenvalue

$$E^m_{2,2,4} = 6J\left(h^4_{12} + h^4_{34}\right) - g\mu_B Bm.$$

C. Model parameters

The overall description of the magnetic properties of Ni_4Mo_{12} obtained with the aid of (3.1) requires 14 parameters. Four field-independent parameters, i.e., J, c^1_{12}, c^2_{12}, and c_{34}, are determined via the neutron spectroscopic analysis, see, e.g., Ref. [42]. The other ten parameters, denoted commonly by "h", account for the indirect influence of the externally applied magnetic field onto the correlation functions. Their values can be determined from the magnetization and the magnetic susceptibility measurements. Thus, one could expect that for

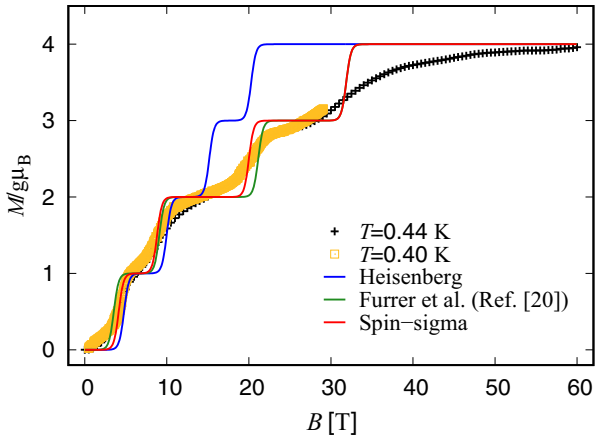

FIG. 3. Magnetization steps in the molecular magnet Ni_4Mo_{12}. The yellow and black symbols depict the experimental data from Ref. [17]. The solid blue and red lines represent the calculated magnetization assuming the isotropic Heisenberg and Hamiltonian (2.1), respectively, with $J = 0.325$ meV. The green line represents the magnetization curve obtained with the aid of model (3.5) proposed in Ref. [20]. All calculations are performed at $T = 0.44$ K and $g = 2.25$. The fitted parameters of the Hamiltonian (2.1) are given in Table I.

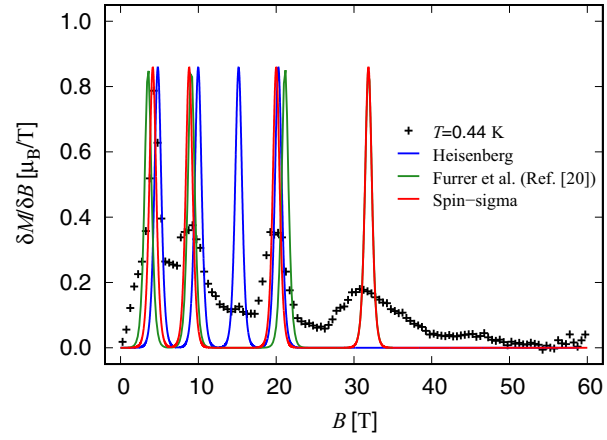

FIG. 4. Differential magnetization. The experimental data from Ref. [17] are depicted with black symbols. The calculated differential magnetization for the isotropic Heisenberg and Hamiltonian (2.1), with $J = 0.325$ meV, are shown by blue and red lines, respectively. The green line is associated to model (3.5) used in Ref. [20]. All results are obtained at $T = 0.44$ K and $g = 2.25$. The parameters entering into (2.1) are provided in Table I.

small magnitudes of the external magnetic field the proposed parameters will tend to one.

We would like to point out that the parameters in (2.1) are intended to capture a particular degeneracy of the initial energy spectrum obtained within the framework of the applied variational method briefly discussed in Sec. II A and in more detail in Ref. [42]. This degeneracy arises from the probability of observing different distributions of all electrons involved in the exchange processes. It is influenced by the presence of an externally applied magnetic field and it decreases exponentially with increasing temperature. Thus, the Hamiltonian in (2.1) is an effective model for studying low-temperature properties when $T \to 0$ and any attempt of tuning the "h" parameters to high temperature measurements would lead to erroneous results. Thereby the low-temperature and high-field magnetization measurements play a crucial role in extracting precise information on the values of the aforementioned parameters.

Using the Hamiltonian (3.1) we have computed the magnetization, differential magnetization, and low-field susceptibility shown on Figs. 3, 4, and 5, respectively. The values of the parameters J, c^1_{12}, c^2_{12}, and c_{34} are determined according to the neutron spectroscopy analysis reported in Ref. [42] and are listed in Table I along with the values for the field parameters discussed in Sec. III B.

These values allow us to reproduce the experimentally observed four magnetization steps found at 4.5, 8.9, 20.1, and 32 T of Ref. [17]. The values of both parameters h^0_{ij} and h^1_{ij} indicate the low-field dependence of Ni_4Mo_{12} molecule. On the other hand, the values of quintet and septet field parameters, corresponding to the domain $10 \leqslant B \leqslant 30$, significantly differ form h^0_{ij} and h^1_{ij}. Moreover, a pronounced jump is exhibited between h^2_{ij} and h^3_{ij}. According to the used formalism such results are a signal for relatively important electrons orbital contributions. As a result, independently of the Zeeman splitting the molecule exhibits shifting of the energy levels, see Fig. 2.

D. Comparison to model H_{2a} of Ref. [20]

To describe the magnetic spectrum of the compound Ni_4Mo_{12}, in Ref. [20] several models based on the conventional Heisenberg interaction among localized spins were proposed. One of them tried to accommodate at the best the distorted crystalline structure of the considered molecular

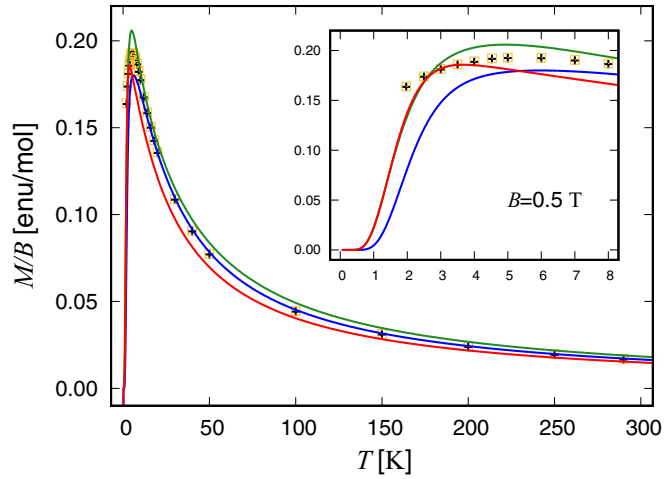

FIG. 5. Low-field susceptibility. The experimental points from Ref. [17] are in yellow and black. The blue and red lines represent the theoretical calculations, where the respective Hamiltonians are the isotropic Heisenberg and Hamiltonian (2.1) with $J = 0.325$ meV. The results obtained with the aid of model (3.5) constructed in Ref. [20] are depicted by a green line. All calculations are performed with respect to the values $B = 0.5$ T and $g = 2.25$. The values of all field parameters for (2.1) are given in Table I.

magnet. Taking into account our convention, the named model involving anisotropic in space spin-spin interaction and an axial single-ion anisotropy, reads

$$H_{2a} = 2J(\hat{\mathbf{s}}_3 \cdot \hat{\mathbf{s}}_1 + \hat{\mathbf{s}}_3 \cdot \hat{\mathbf{s}}_2 + \hat{\mathbf{s}}_3 \cdot \hat{\mathbf{s}}_4 + \hat{\mathbf{s}}_1 \cdot \hat{\mathbf{s}}_2) + 2J'(\hat{\mathbf{s}}_4 \cdot \hat{\mathbf{s}}_1 + \hat{\mathbf{s}}_4 \cdot \hat{\mathbf{s}}_2) + D\sum_{i=1}^{4}\left(\mathrm{s}_i^z\right)^2. \tag{3.5}$$

Here, the parameters $J = 0.2517$ meV, $J' = 0.5723$ meV, and $D = 0.2025$ meV are determined by fitting to the relevant experimental data.

To compare our results, we computed the magnetization and the susceptibility with the aid of Hamiltonian (3.5). The results for the associated physical quantities are depicted with a green line on Figs. 3, 4, and 5. Notice that at weak external magnetic field, Hamiltonians (2.1) and (3.5) lead to slightly different results, while at strong fields ($B > 25$ T) the corresponding curves are indiscernible, see Figs. 3 and 4. On Fig. 5, we show the temperature dependence of the low-field susceptibility at $B = 0.5$. We see clearly that at low temperatures our model (2.1) fits better to experimental results than the Heisenberg Hamiltonian (3.5) with single-ion anisotropy.

IV. CONCLUSION

In order to study the magnetization and magnetic susceptibility of the magnetic molecule Ni_4Mo_{12} we extended the introduced in Ref. [42] post-Hartree-Fock method, based on the molecular orbital theory, by accounting for the orbital contributions of the electrons to the intrinsic molecular field and found all electrons' correlations as field dependent [43]. We calculated the effect of externally applied magnetic field on the electrons' correlations with the aid of the effective spin-sigma bilinear form (2.1) via the field parameters described in Sec. II B. This allowed us to reproduce the behavior of the magnetization, differential magnetization and low-field susceptibility data reported in Ref. [17]. As it is shown on Figs. 3, 4, and 5 the obtained results are consistent with the available experimental data.

The values of all parameters entering the theory are presented in Table I. The role of the "h" parameters is to detect any variations in the zero-field energy spectrum induced from the externally applied magnetic field. Thus, as the magnitude of the external magnetic field increases, the energy sequence alters making the molecule more resistive to the applied external action. Consequently, one needs to input more magnetic energy in order to magnetize the molecule, Fig. 3. This process is also visible from the susceptibility measurements, see Fig. 4. The gaps become wider increasing the magnitude of the external magnetic field and hence making the Ni tetramer less susceptible. On both Figs. 3 and 4 the described effect is pronounced in the interval 10–30 T.

This process is also imprinted in the diagram shown on Fig. 2. The triplet and quintet energy levels are very close to each other and almost indistinguishable. As a consequence the triplet step, i.e., after 5 and 8 T, is not as wide as the upper steps. On the other hand, the quintet and septet energy levels are separated by a larger energy gap, which explains the extent of the quintet step. The same principle defines the width of septet plateau.

The approach used of the present study is applicable to any isolated nanomagnetic unit with a set of magnetic centers interacting by one or more complex intermediate bridges. The microscopic model in (2.1) rests on the multiconfiguration self consistent field method based on the molecular orbital theory. Therefore, it is aimed to capture all magnetic features originating from the electrons' delocalization and their distribution along the exchange bridges of a finite-sized magnetic complex. It may be of great value since a nontrivial bridging structure favors a multitude of electrons' distributions leading to a number of magnetic excitations that do not result from spin-orbit coupling processes nor from the existence of conducting bands. Furthermore, such bridging structure also favors strong field dependent electrons' correlations arising form the orbital contribution of each delocalized electron included in the exchange processes. In that respect neither of the known conventional effective spin models possess an adequate parametrization scheme. Moreover, any attempt to tune the exchange parameters from any such model lead to an incomplete energy spectrum making the former inconvenient and thus inadequate. To conclude, for nanomagnets with trivial bonding bridges and localized electrons the Hamiltonian in (2.1) naturally reduces to the Heisenberg model.

ACKNOWLEDGMENTS

The authors are indebted to Professor N. S. Tonchev, Professor N. Ivanov for very helpful discussions, and to Professor J. Schnack for providing us with the experimental data used in Figs. 3, 4, and 5. This work was supported by the Bulgarian National Science Fund under Grant No. DN08/18 and the National program "Young scientists and postdoctoral researchers" approved by DCM 577, 17.08.2018.

[1] A. Hernando, *Nanomagnetism* (Springer Netherlands, Dordrecht, 1993).

[2] D. Gatteschi, R. Sessoli, and J. Villain, *Molecular Nanomagnets* (Oxford University Press, Oxford, 2006).

[3] L. Bogani and W. Wernsdorfer, Molecular spintronics using single-molecule magnets, Nature Mater. **7**, 179 (2008).

[4] F. Nasirpouri and A. Nogaret, *Nanomagnetism and Spintronics: Fabrication, Materials, Characterization and Applications* (World Scientific, Singapore, 2011).

[5] H. Chamati, Theory of phase transitions: From magnets to biomembranes, Adv. Planar Lipid Bilayers Liposomes **17**, 237 (2013).

[6] S. T. Liddle and J. van Slageren, Improving f-element single molecule magnets, Chem. Soc. Rev. **44**, 6655 (2015).

[7] A. Caneschi, D. Gatteschi, R. Sessoli, A. L. Barra, L. C. Brunel, and M. Guillot, Alternating current susceptibility, high field magnetization, and millimeter band EPR evidence for a ground

S=10 state in $[Mn_{12}O_{12}(CH_3COO)_{16}(H_2O)_4] \cdot 2CH_3COOH \cdot 4H_2O$, J. Am. Chem. Soc. **113**, 5873 (1991).

[8] R. Sessoli, D. Gatteschi, A. Caneschi, and M. A. Novak, Magnetic bistability in a metal-ion cluster, Nature (London) **365**, 141 (1993).

[9] Z. H. Jang, A. Lascialfari, F. Borsa, and D. Gatteschi, Measurement of the Relaxation Rate of the Magnetization in $Mn_{12}O_{12}$-Acetate using Proton NMR Echo, Phys. Rev. Lett. **84**, 2977 (2000).

[10] N. Regnault, Th. Jolicœur, R. Sessoli, D. Gatteschi, and M. Verdaguer, Exchange coupling in the magnetic molecular cluster Mn_{12}Ac, Phys. Rev. B **66**, 054409 (2002).

[11] V. V. Mazurenko, Y. O. Kvashnin, F. Jin, H. A. De Raedt, A. I. Lichtenstein, and M. I. Katsnelson, First-principles modeling of magnetic excitations in Mn_{12}, Phys. Rev. B **89**, 214422 (2014).

[12] A. Chiesa, T. Guidi, S. Carretta, S. Ansbro, G. A. Timco, I. Vitorica-Yrezabal, E. Garlatti, G. Amoretti, R. E. P. Winpenny, and P. Santini, Magnetic Exchange Interactions in the Molecular Nanomagnet Mn_{12}, Phys. Rev. Lett. **119**, 217202 (2017).

[13] W. Wernsdorfer, Quantum phase interference and parity effects in magnetic molecular clusters, Science **284**, 133 (1999).

[14] S. Maccagnano, R. Achey, E. Negusse, A. Lussier, M. Mola, S. Hill, and N. Dalal, Single crystal EPR determination of the spin Hamiltonian parameters for Fe_8 molecular clusters, Polyhedron **20**, 1441 (2001).

[15] T. Leviant, A. Keren, E. Zeldov, and Y. Myasoedov, Quantum ignition of deflagration in the Fe_8 molecular magnet, Phys. Rev. B **90**, 134405 (2014).

[16] M. Yaari and A. Keren, Temperature changes of the Fe_8 molecular magnet during its spin reversal process, Phys. Rev. B **95**, 174435 (2017).

[17] J. Schnack, M. Brüger, M. Luban, P. Kögerler, E. Morosan, R. Fuchs, R. Modler, H. Nojiri, R. C. Rai, J. Cao, J. L. Musfeldt, and X. Wei, Observation of field-dependent magnetic parameters in the magnetic molecule $\{Ni_4Mo_{12}\}$, Phys. Rev. B **73**, 094401 (2006).

[18] V. V. Kostyuchenko, Non-Heisenberg exchange interactions in the molecular magnet Ni_4Mo_{12}, Phys. Rev. B **76**, 212404 (2007).

[19] J. Nehrkorn, M. Höck, M. Brüger, H. Mutka, J. Schnack, and O. Waldmann, Inelastic neutron scattering study and Hubbard model description of the antiferromagnetic tetrahedral molecule Ni_4Mo_{12}, Eur. Phys. J. B **73**, 515 (2010).

[20] A. Furrer, K. W. Krämer, T. Strässle, D. Biner, J. Hauser, and H. U. Güdel, Magnetic and neutron spectroscopic properties of the tetrameric nickel compound $[Mo_{12}\ O_{28}(\mu_2\text{-}OH)_9(\mu_2\text{-}OH)_3\{Ni(H_2O)_3\}_4] \cdot 13H_2O$, Phys. Rev. B **81**, 214437 (2010).

[21] W. Hübner, Y. Pavlyukh, G. Lefkidis, and J. Berakdar, Magnetism of a four-center transition-metal cluster revisited, Phys. Rev. B **96**, 184432 (2017).

[22] R. A. Klemm and D. V. Efremov, Single-ion and exchange anisotropy effects and multiferroic behavior in high-symmetry tetramer single-molecule magnets, Phys. Rev. B **77**, 184410 (2008).

[23] Z. Salman, A. Keren, P. Mendels, V. Marvaud, A. Scuiller, M. Verdaguer, J. S. Lord, and C. Baines, Dynamics at $T \to 0$ in half-integer isotropic high-spin molecules, Phys. Rev. B **65**, 132403 (2002).

[24] S. Blundell, F. Pratt, T. Lancaster, I. Marshall, C. Steer, W. Hayes, T. Sugano, J.-F. Letard, A. Caneschi, D. Gatteschi, and S. Heath, μ SR study of organic systems: ferromagnetism, antiferromagnetism, the spin-crossover effect, and fluctuations in magnetic nanodiscs, Physica B **326**, 556 (2003).

[25] J. Ummethum, J. Nehrkorn, S. Mukherjee, N. B. Ivanov, S. Stuiber, T. Strässle, P. L. W. Tregenna-Piggott, H. Mutka, G. Christou, O. Waldmann, and J. Schnack, Discrete antiferromagnetic spin-wave excitations in the giant ferric wheel Fe_{18}, Phys. Rev. B **86**, 104403 (2012).

[26] G. A. Timco, S. Carretta, F. Troiani, F. Tuna, R. J. Pritchard, C. A. Muryn, E. J. L. McInnes, A. Ghirri, A. Candini, P. Santini, G. Amoretti, M. Affronte, and R. E. P. Winpenny, Engineering the coupling between molecular spin qubits by coordination chemistry, Nature Nanotechnol. **4**, 173 (2009).

[27] C. J. Wedge, G. A. Timco, E. T. Spielberg, R. E. George, F. Tuna, S. Rigby, E. J. L. McInnes, R. E. P. Winpenny, S. J. Blundell, and A. Ardavan, Chemical Engineering of Molecular Qubits, Phys. Rev. Lett. **108**, 107204 (2012).

[28] S. Sanna, P. Arosio, L. Bordonali, F. Adelnia, M. Mariani, E. Garlatti, C. Baines, A. Amato, K. P. V. Sabareesh, G. Timco, R. E. P. Winpenny, S. J. Blundell, and A. Lascialfari, Low-field spin dynamics of Cr_7Ni and Cr_7Ni–Cu–Cr_7Ni molecular rings as detected by μSR, Phys. Rev. B **96**, 184403 (2017).

[29] A. Stebler, H. U. Guedel, A. Furrer, and J. K. Kjems, Intra- and intermolecular interactions in $[Ni_2(ND_2C_2H_2ND_2)_4Br_2]Br_2$. Study by inelastic neutron scattering and magnetic measurements, Inorg. Chem. **21**, 380 (1982).

[30] J. J. Borrás-Almenar, J. M. Clemente-Juan, E. Coronado, and B. S. Tsukerblat, High-Nuclearity Magnetic Clusters: Generalized Spin Hamiltonian and Its Use for the Calculation of the Energy Levels, Bulk Magnetic Properties, and Inelastic Neutron Scattering Spectra, Inorg. Chem. **38**, 6081 (1999).

[31] M. Matsuda, K. Kakurai, A. A. Belik, M. Azuma, M. Takano, and M. Fujita, Magnetic excitations from the linear Heisenberg antiferromagnetic spin trimer system $A_3Cu_3(PO_4)_4$ (A = Ca, Sr, and Pb), Phys. Rev. B **71**, 144411 (2005).

[32] D. Procissi, A. Lascialfari, E. Micotti, M. Bertassi, P. Carretta, Y. Furukawa, and P. Kögerler, Low-energy excitations in the $S=\frac{1}{2}$ molecular nanomagnet $K_6[V^{IV}_{15}\ As_6\ O_{42}(H_2O)] \cdot 8H_2O$ from proton NMR and μ SR, Phys. Rev. B **73**, 184417 (2006).

[33] J. Lago, E. Micotti, M. Corti, A. Lascialfari, A. Bianchi, S. Carretta, P. Santini, D. Procissi, S. H. Baek, P. Kögerler, C. Baines, and A. Amato, Low-energy spin dynamics in the giant keplerate molecule $\{Mo_{72}Fe_{30}\}$: A muon spin relaxation and ^{1}H NMR investigation, Phys. Rev. B **76**, 064432 (2007).

[34] J. Zhao, D. T. Adroja, D.-X. Yao, R. Bewley, S. Li, X. F. Wang, G. Wu, X. H. Chen, J. Hu, and P. Dai, Spin waves and magnetic exchange interactions in $CaFe_2As_2$, Nature Phys. **5**, 555 (2009).

[35] M. Ghosh, M. Majumder, K. Ghoshray, and S. Banerjee, Magnetic properties of the spin trimer compound $Ca_3Cu_2Mg(PO_4)_4$ from susceptibility measurements, Phys. Rev. B **81**, 094401 (2010).

[36] E. Minamitani, N. Takagi, and S. Watanabe, Model Hamiltonian approach to the magnetic anisotropy of iron phthalocyanine at solid surfaces, Phys. Rev. B **94**, 205402 (2016).

[37] Md. M. Seikh, V. Caignaert, O. Perez, B. Raveau, and V. Hardy, Single-ion and single-chain magnetism in triangular spin-chain oxides, Phys. Rev. B **95**, 174417 (2017).

[38] X.-H. Zhao, L.-D. Deng, Y. Zhou, D. Shao, D.-Q. Wu, X.-Q. Wei, and X.-Y. Wang, Slow magnetic relaxation in one-dimensional azido-bridged Co^{ii} complexes, Inorg. Chem. **56**, 8058 (2017).

[39] A. Müller, C. Beugholt, P. Kögerler, H. Bögge, S. Bud'ko, and M. Luban, $[Mo^{V}_{12}O_{30}(\mu_2\text{-}OH)_{10}H_2\{Ni^{II}(H_2O)_3\}_4]$, a highly symmetrical ε-keggin unit capped with four Ni^{II} centers: Synthesis and magnetism, Inorg. Chem. **39**, 5176 (2000).

[40] M. Georgiev and H. Chamati, Magnetic exchange in spin clusters, AIP Conf. Proc. **2075**, 020004 (2019).

[41] M. Georgiev and H. Chamati, Magnetic excitations in the trimeric compounds $A_3Cu_3(PO_4)_4$ (A = Ca, Sr, Pb), C.R. Acad. Bulg. Sci. **72**, 29 (2019).

[42] M. Georgiev and H. Chamati, Magnetic excitations in molecular magnets with complex bridges: The tetrahedral molecule Ni_4Mo_{12}, Eur. Phys. J. B **92**, 93 (2019).

[43] M. Georgiev and H. Chamati (under preparation).

[44] B. O. Roos, The Complete Active Space Self-Consistent Field Method and its Applications in Electronic Structure Calculations, in *Advances in Chemical Physics*, edited by K. P. Lawley (John Wiley & Sons, Inc., Hoboken, 2007), pp. 399–445.

[45] P. G. Szalay, T. Müller, G. Gidofalvi, H. Lischka, and R. Shepard, Multiconfiguration self-consistent field and multireference configuration interaction methods and applications, Chem. Rev. **112**, 108 (2012).

[46] M. Vonci, M. J. Giansiracusa, W. Van den Heuvel, R. W. Gable, B. Moubaraki, K. S. Murray, D. Yu, R. A. Mole, A. Soncini, and C. Boskovic, Magnetic excitations in polyoxotungstate-supported lanthanoid single-molecule magnets: An inelastic neutron scattering and *ab initio* study, Inorg. Chem. **56**, 378 (2017).

[47] I. Fleming, *Molecular Orbitals and Organic Chemical Reactions* (Wiley, Chichester, 2009).

[48] T. A. Albright, J. K. Burdett, and M.-H. Whangbo, *Orbital Interactions in Chemistry* (John Wiley & Sons, Inc., Hoboken, 2013).